

Design of 3-axis Capacitive Low-Gravity MEMS Accelerometer with Zero Cross-Axis Sensitivity in a Commercial Process

A. Merdassi and V. P Chodavarapu

Department of Electrical & Computer Engineering, McGill University
3480 University Street, Montreal, Canada H3A0E9
Emails: adel.merdassi@mail.mcgill.ca, vamsy.chodavarapu@mcgill.ca
Phone: (514) 398 3118; Fax: (514) 398 4470

ABSTRACT

We present the design and fabrication of a 3-axis capacitive accelerometer that is developed using SOIMUMPS, which is a commercial multi-user process available from MEMSCAP. The accelerometer is designed to measure ultra-low acceleration with a range of $\pm 100\text{mg}$. We introduce a new technique to reduce or eliminate the cross-axis sensitivity based on the use of decoupled frames and appropriate mechanical springs that are sensitive for each specific axis. The proposed accelerometer device requires two post-fabrication processing steps that improve the fabrication device yield and for strategic design of the mechanical springs. The two steps include using Deep Reactive Ion-Etching (DRIE) to etch the bulk silicon for releasing the proof mass structure using oxide as masking layer and second, to pattern the multiple frame structures for multi-axis operation. The fabricated accelerometer device has an initial capacitance of approximately 1pF with a gap between inter-digitated comb fingers of $3\mu\text{m}$. The device sensitivity is 50fF/g with a resolution of $0,08\text{mg}/\sqrt{\text{Hz}}$.

Keywords: Low-g accelerometer, 3-axis accelerometer, Decoupled frames, SOIMUMPS, Zero cross-axis sensitivity, MEMS inertial sensor, Capacitance sensing.

1 INTRODUCTION

There is a significant interest to develop multi-axis, high sensitivity and high resolution accelerometers in milli-gravity range for human and animal wearable sensor applications, human-computer interfaces, and biomedical applications [1]. Many implementations described previously in literature use bulk micromachining to fabricate a large proof mass that is sensitive to accelerations in ultra-low gravity range [2, 3]. However, the use of bulk micromachining makes it difficult to design fully integrated single-chip multi-axis accelerometers. Surface micromachining provides more flexibility in developing integrated 3-axis or multi-axis accelerometers by using adequate springs that avoid the measurement errors due to cross-axis sensitivity that arises due to the orthogonal-oriented accelerations [4]. Here, we present a novel

integrated 3-axis accelerometer for ultra-low g measurements with zero cross-axis sensitivity using a commercial process. The accelerometer is developed using SOIMUMPS, which is a commercial multi-user process available from MEMSCAP. Post-fabrication processing of the accelerometer devices using Deep Reactive Ion-Etching (DRIE) is required to improve the fabrication device yield and for strategic design of mechanical springs.

We employ capacitive transduction mechanism which provides high reliability, low temperature sensitivity, low drift, and low power consumption. Like other capacitive inertial MEMS sensors, the proposed accelerometer makes use of suspended proof mass structure undergoing force stimulus due to the applied acceleration. We obtain high sensitivity based on using a large proof mass attached to mechanical springs with low stiffness. The capacitance data acquisition is based on using the Analog Devices AD7150 circuit board which allows a detection sensitivity of 1fF . In Section 2, an overview on the working principle is presented, the detailed accelerometer design is presented in Section 3 and the post-fabrication process of the accelerometer is presented in Section 4.

2 3-AXIS ACCELEROMETER DESIGN AND WORKING PRINCIPLE

The working principle for most inertial MEMS sensors is based on forced vibration of a mechanical structure, which is modeled as proof mass-spring mechanical system undergoing inertial force, due to the applied acceleration. The mechanical sensitivity can be deduced from the transfer function, $H(\omega)$, that relates the frame displacement to the proof mass displacement as given by Equation (1) [5].

$$H(\omega) = \frac{Z}{X} = \frac{\omega^2}{\omega_n^2 \sqrt{\left(1 - \frac{\omega^2}{\omega_n^2}\right)^2 + \left(2\xi \frac{\omega}{\omega_n}\right)^2}} \quad (1)$$

where, damping ratio, $\xi = \frac{b}{b_r} = \frac{b}{2\sqrt{km}}$ is the ratio

between the damping coefficient, b , and the critical damping coefficient, b_r , and $Z = Y - X$ is the relative

displacement of the comb-shaped electrodes attached to the proof mass with respect to the fixed comb-shaped detection electrodes attached to a frame. The damping ratio is typically much smaller than unity and the frequency range of the sensor is equivalent to the frequency interval where the transfer function is quasi constant which leads to constant sensitivity of the accelerometer. Thus, the transfer function at zero frequency represents the mechanical sensitivity, S_{mech} , and is given by Equation (2).

$$S_{mech} = \frac{\Delta x}{\Delta a} = \frac{1}{\omega_0^2} \quad (2)$$

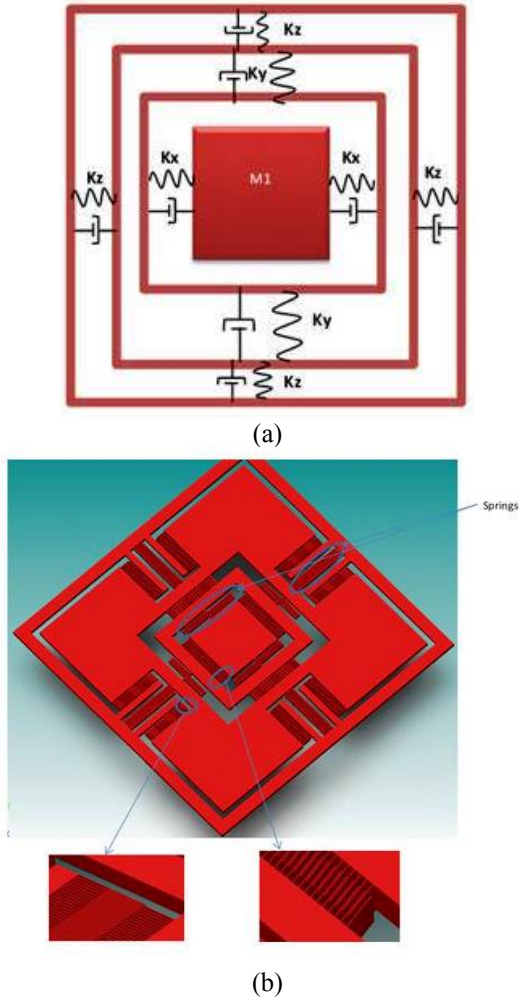


Figure 1: (a) Accelerometer topology using three different springs for the three axes and (b) 3D model of the proposed accelerometer device

The displacement of the proof mass can be converted into electrical signal by means of capacitive transduction. In our case, we used differential capacitance measurements to improve the sensitivity and to reduce the offset error. The electrical sensitivity, S_{elec} , is given by the ratio between the capacitance change and the displacement of the proof mass

with respect to the frame and is given by, $S_{elec} = \frac{\Delta C}{\Delta x}$,

where, the initial capacitance, C , is given by, $C = \frac{\epsilon S}{d}$.

Thus, the total sensitivity of the sensor is given by, $S_{sens} = S_{mech} S_{elec}$. An important parameter of the accelerometer is the cross-axis sensitivity which is defined as the ratio of the x_i deflection caused by an orthogonal acceleration, a_i and the deflection caused by the same acceleration applied in the x direction [1]. The cross-axis sensitivity is given by Equation (3).

$$S_{xx_i} \Big|_{a_x=a_i} = \frac{k_{xx_i}}{k_x} \left(\frac{\omega_0}{\omega_i} \right)^2 \quad (3)$$

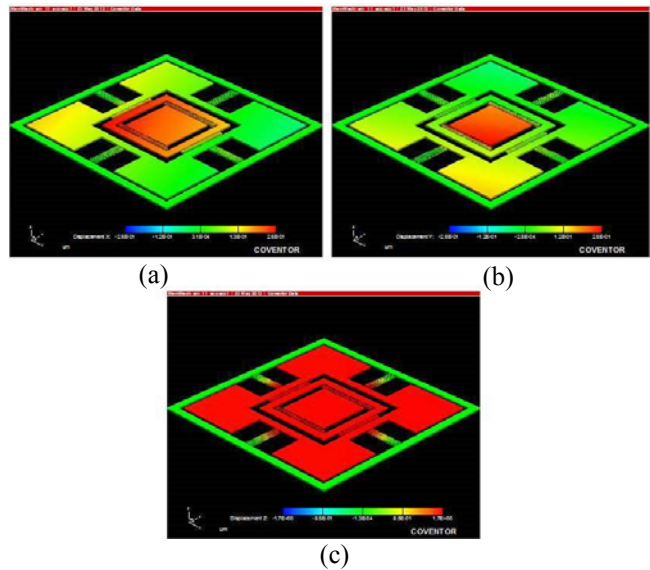


Figure 2: Displacements of the proof mass for a full range measurement along (a) X-axis, (b) Y-axis, and (c) Z-axis

2.1 Mechanical Design

An important design aspect for the low-g accelerometer is to increase the mechanical sensitivity to get a reasonable displacement when applying acceleration on the order of $\pm 100\text{mg}$. This can be done by increasing the proof mass size or by decreasing the stiffness of the springs that support the proof mass by connecting multiple unit springs in series. Here, we used serpentine type mechanical springs and an estimate value for the total spring stiffness in the

present case is given by, $k_{spring} = 2 \frac{k_{unit}}{N}$, where, $N=4$

along X-axis and $N=6$ along Y-axis and $k_{unit} = 12 \frac{EI}{L^3}$,

where, I is the moment inertia around Z-axis. To eliminate the problem of the cross-axis sensitivity, the proposed

design was based on using different frames that decouples the modes along the different axis. Thus, we used two frames and strategic design of the springs to determine movements along the different axis as shown in Figure 2.

2.2 Electrical Design

The capacitance transduction for detecting in-plane acceleration is based on the variation of the gap between the comb shaped electrodes attached to the proof-mass and fixed comb-shaped detection electrodes attached to the frame. For the intended milli-g acceleration range, we designed the movement of the proof-mass structure to reach approximately 8% of the full gap between the comb electrodes as shown in Figure 3. This choice of percentage provides a linear response of the capacitance signal for the acceleration range. For detecting out-of-plane acceleration along Z-axis, the height of the comb electrodes controls the linearity of the capacitance transduction.

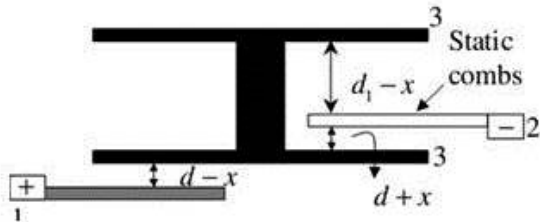


Figure 3: Differential capacitance arrangement for the comb electrodes [5]

The capacitance change along X- or Y- axis is given by, $\Delta C = C_0 \frac{d_1 - d}{dd_1} \Delta x$, where, the estimated ratio

between d and d_1 , which is used to increase the capacitance signal variation, is set at 2. The capacitance signal change

along Z-axis is given by, $\Delta C = C_0 \frac{\Delta h}{h}$, where, h is the

height of each comb finger electrode. The device sensitivity relies on the variation in the capacitance signal due to the applied acceleration and is given by,

$$S_{sens} = \frac{\Delta C}{\Delta a} = C_0 \frac{m}{k_T} \frac{d_1 - d}{dd_1}$$

for in-plane acceleration

$$\text{and } S_{sens} = \frac{\Delta C}{\Delta a} = C_0 \frac{m}{k_T h}$$

for out-of-plane acceleration.

3 DEVICE MODELING AND SIMULATION

We simulated the performance of the accelerometer device using CoventorWare finite element modeling software. The simulation results provide the relationship between the variations in capacitance signal as a function of the applied acceleration. Two types of simulation were

performed; first, mechanical simulation illustrates the displacement values with respect to applied acceleration as shown in Figure 4. Second, we simulated the calibration response for the accelerometer device as shown in Figure 5. In theory, the maximum displacement to be reached is approximately $0.25 \mu\text{m}$ which represents 8% of the full $3 \mu\text{m}$ gap between the comb electrodes. We maintain the same percentage along Z-axis that is $2 \mu\text{m}$ out of total $25 \mu\text{m}$ height of comb electrodes. Model analysis was performed to study the dynamic behavior of the accelerometer to deduce the frequency bandwidth of the device. The three modes along X-, Y- and Z- axis are fixed approximately at 389Hz, 385Hz and 122 Hz respectively.

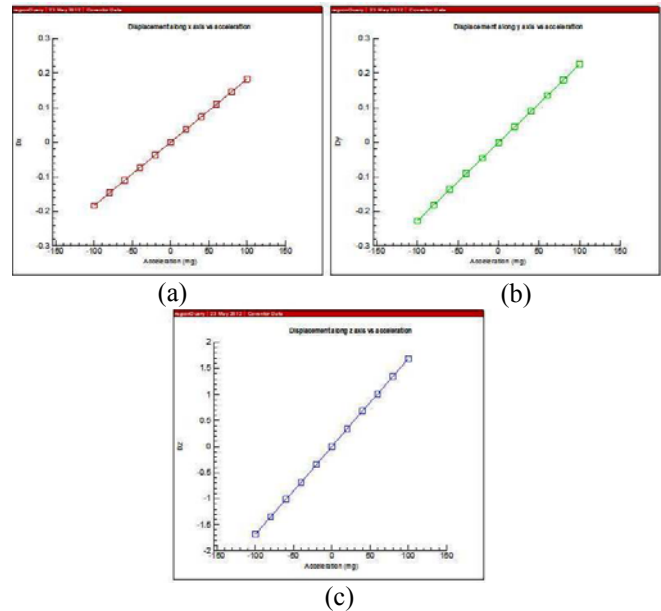


Figure 4: Displacements curves for the different axis along (a) X-axis, (b) Y-axis, and (c) Z-axis

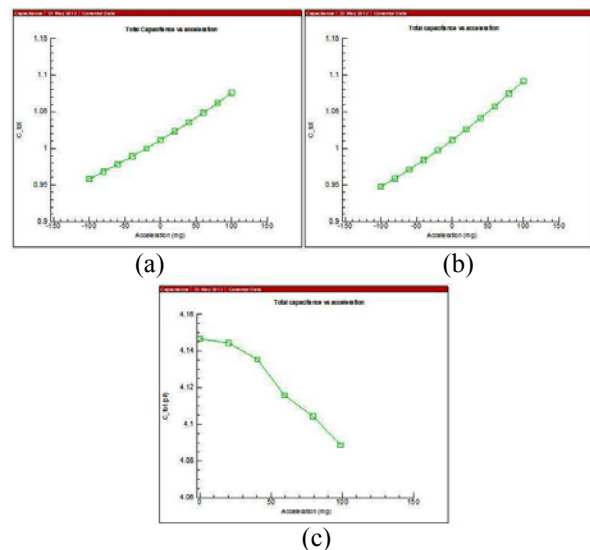


Figure 5: Calibration curves for the different axis along (a) X-axis, (b) Y-axis, and (c) Z-axis

The simulation of the calibration response aims to provide relationship between the applied acceleration and its associated capacitance variation. This response provides information related to the sensor sensitivity. The response has a nonlinear profile and therefore, statistical processing based on the least square method is used to deduce the sensitivity by extracting its estimated coefficients. Table 1 shows the numerical results given by the simulation results.

Table 1: Mechanical and electrical simulation parameters of the accelerometer device

Axis	X	Y	Z
Mechanical sensitivity S_{mech} ($\mu\text{m/g}$)	1.83	2.25	17
D_{max} (μm)	0.183	0.225	1.7
Total spring constant K_T (10^{-1} N/m)	1.22	1.36	1.8
Initial capacitance C_0 (10^{-2} pF)	50.56	50.56	51.83
Total capacitance C_{tot} (pF)	1.011	1.011	1.03
$\Delta C_{TOT_{max}}$ (fF)	69.4	85.32	70.5
Sensitivity S_{sens} (fF/g)	58.6	71.85	15.38
Dimensions (μm^3)	2700x2700x25 μm		

4 FABRICATION PROCESS

The accelerometer is fabricated using SOIMUMPS, which is a commercial multi-user process available from MEMSCAP by creating the central proof mass structure that is suspended by mechanical springs. The SOIMUMPS process uses Silicon-on-Insulator (SOI) wafer and begins by patterning the device layer of the SOI wafer to form the proof mass, frames, and serpentine springs. The devices are then processed using a DRIE procedure by dry etching from back side to release the central suspended proof mass. This step is followed by dry etching of the oxide layer using HF vapor dry etch process and finally a metallization procedure to create the electrode contacts and the wire-bonding pads. The devices are then post-fabrication processed using DRIE procedure from the back side to release all the suspended proof-masses (within the two frames). This is performed using PECVD oxide as mask layer. The patterning of the oxide mask is performed by photolithography process and dry etching by means of CHF_3 etchant gas. The final step is to pattern the frames by photolithography and DRIE etching process to leave a silicon layer (handle layer of SOI wafer) of $20\mu\text{m}$. Figure 6(a) and 6(b) show the final design and microphotograph of post-fabrication processed accelerometer device, respectively.

5 CONCLUSIONS

We presented the design and fabrication of a 3-axis accelerometer for ultra-low g measurements with a range of

$\pm 100\text{mg}$ with zero cross-axis sensitivity using a commercial SOIMUMPS process. The proposed accelerometer device requires two post-fabrication processing steps that improve the fabrication device yield and for strategic design of the mechanical springs. We are currently working towards characterizing the performance of the accelerometer device.

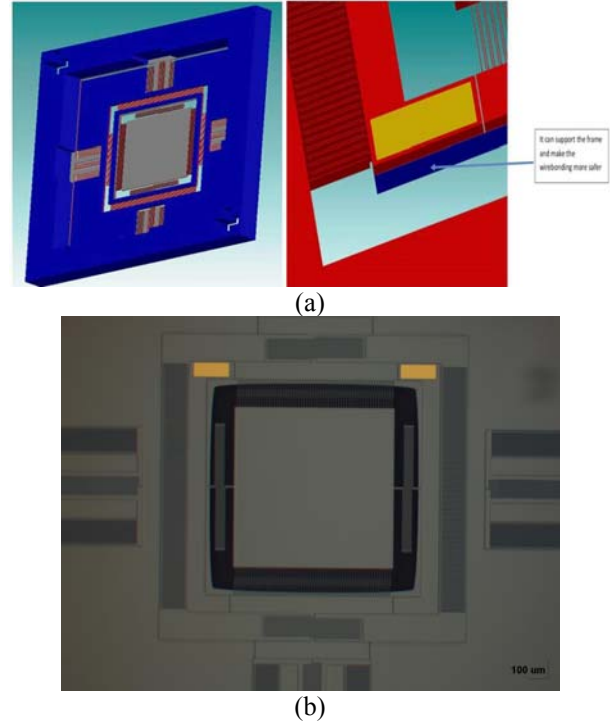


Figure 6: (a) 3D view of the accelerometer from the back side along with its frame structure. (b) Microphotograph of the fabrication accelerometer device

REFERENCES

- [1] V. Kampe, "Accelerometers" in Inertial MEMS Principle and Practices, 1st ed., New York: Ed. Cambridge University, pp. 283-357, 2011.
- [2] R. A. Dias, L. Mol, R. F. Wolffenbuttel, E. Cretu, and L. A. Rocha, "Design of a Time-Based Micro-g Accelerometer", IEEE Sensors Journal, vol. 11, pp. 1677-1683, 2011.
- [3] J. Chae, H. Kulah and K. Najafi, "A monolithic three axis micro-g micromachined silicon capacitive accelerometer", Journal of Micromechanical systems, vol. 14, pp. 202-203, 2005.
- [4] H. Farahani, J. K. Mills and W. L. Cleghorn, "Design, fabrication and analysis of micromachined high sensitivity and 0% cross-axis sensitivity capacitive accelerometers", Microsystem Technologies Journal, vol. 15, pp. 1815-1826, 2009.
- [5] G. Krishnan, C. U. Kshirsagar, G. K. Ananthasuresh, and N. Bhat, "Micromachined High-Resolution Accelerometers", The Journal of the Indian Institute of Science, vol. 87, pp. 333-361, 2007.